

Trace Moisture Detection Using Continuous-Wave Cavity Ring-Down Spectroscopy

John B. Dudek,[†] Peter B. Tarsa, Armando Velasquez,[‡] Mark Wladyslawski, Paul Rabinowitz, and Kevin K. Lehmann*

Department of Chemistry, Princeton University, Princeton, New Jersey 08544

We have developed an instrument to measure trace concentrations of small hydride species in gases using continuous-wave cavity ring-down spectroscopy with near-infrared diode laser excitation. An rms baseline equivalent absorbance of $9.2 \times 10^{-11} \text{ cm}^{-1}/\sqrt{n}$ is found, where n is the number of ring-down transients. When the 1396.376-nm absorption line of water is used, this corresponds to a noise equivalent moisture concentration in nitrogen gas of 68 pptv/ \sqrt{n} . Water vapor concentration is detected over a range extending from 3 to 1000 ppbv and found to depend linearly on the concentration as determined by a calibrated commercial moisture sensor.

Detection of trace gas species continues to be an important application of spectroscopy.¹ For example, trace levels of moisture and other contaminants in the process gases used for semiconductor chip manufacturing can result in defects in silicon wafers.² Absorption spectroscopy is particularly attractive for monitoring in such applications because of its high specificity and fast response rate; however, the achievement of sufficient sensitivity in nonlaboratory environments remains a challenge for the detection of ultralow concentrations of contaminant gases. We have developed continuous-wave cavity ring-down spectroscopy (CW-CRDS) as a compact, robust, and modestly priced solution for the near-infrared spectroscopy of small hydride species.^{3, 4}

Our device represents an improvement over the several other methods that have been used for trace moisture detection, including atmospheric pressure ionization mass spectrometry (API-MS) and Fourier transform infrared spectroscopy.^{5–7} These

Table 1. Comparison of Water Detection Techniques

analytical technique	sensitivity to water
API-MS ⁶	1 pptv
FT-IR ⁵	10 ppbv
TTFMS ⁸	40 ppbv
NIR-TDLAS ⁹	4 ppbv
pulsed CRDS ^a	750 pptv
CW-CRDS	70 pptv

^a Extrapolated to 1396.376-nm transition of H₂O from noise equivalent absorbance of HCN reported in ref 20.

approaches are able to achieve detection levels in the parts per trillion by volume (pptv) and low parts per billion by volume (ppbv) range, respectively, but they are not easily portable and require expensive and complicated equipment. Similar detection levels have been reached with some semiconductor laser techniques, such as two-tone frequency modulation spectroscopy (TTFMS) and near-infrared tunable diode laser absorption spectrometry (NIR-TDLAS). Although both benefit from the convenience and cost of diode lasers, they suffer from external absorption interference and high susceptibility to laser amplitude noise.^{8,9} Some reported detection levels achieved with these common techniques are described in Table 1.

The method we employ, cavity ring-down spectroscopy, is a simple and compact technique for trace gas analysis.^{10,11} In contrast to other absorption-based methods, absorbers outside the sample cell do not contribute to CRDS measurement, and laser amplitude noise does not directly affect the stability of the system. CRDS is commonly implemented with pulsed laser sources coupled into a stable optical resonator formed by mirrors of very high intensity reflectivity. When the excitation radiation is switched off, the light intensity in the cavity decreases exponentially in time with a time constant τ , defined as the time to reach $1/e$ of the peak transmission intensity. The decay rate, $\gamma = \tau^{-1}$, is

- (8) Edwards, C. S.; Barwod, G. P.; Gill, P.; Schirmer, B.; Venzke, H.; Melling, A. *Appl. Opt.* **1999**, *38*, 4699–4704.
 (9) Wu, S. Q.; Morishita, J.; Masusaki, H.; Tetsuya, K. *Anal. Chem.* **1998**, *70*, 3315–3321.
 (10) *Cavity-Ringdown Spectroscopy: An Ultratrace-Absorption Measurement Technique*; Busch, K. W., Busch, M. A., Eds.; ACS Symposium Series 720; Oxford University Press: Washington, DC, 1999.
 (11) Paul, J. B.; Scherer, J. J.; O'Keefe, A.; Saykally, R. J. *Laser Focus World* **1997**, *33* (3), 71–80.

* Corresponding author. E-mail: lehmann@princeton.edu.

[†] Present address: Harvard-Smithsonian Center for Astrophysics MS 72, 60 Garden St., Cambridge, MA 02138.

[‡] Present address: 221 Commerce Drive, Montgomeryville, PA 18936-9641.

- (1) Kosterev, A. A.; Tittel, F. K. *IEEE J. Quantum Electron.* **2002**, *38*, 582–591.
 (2) Dance, D. L.; Burghard, R. W.; Markle, R. J. *Microcontamination* **1992**, *10* (5), 21–23, 64.
 (3) Lehmann, K. K. U.S. Patent 5 528 040, 1996.
 (4) Diode Laser Gas Sensing. <http://www.swsciences.com/sensors.html>; accessed 1999.
 (5) Stallard, B. R.; Espinoza, L. H.; Rowe, R. K.; Garcia, M. J.; Niemczyk, T. M. *J. Electrochem. Soc.* **1995**, *142*, 2777–2782.
 (6) Siefering, K.; Berger, H.; Whitlock, W. *J. Vac. Sci. Technol., A* **1993**, *11*, 1593–1597.
 (7) Scott, A. D., Jr.; Hunter, E. J.; Ketkar, S. N. *Anal. Chem.* **1998**, *70*, 1802–1804.

directly proportional to the absorption coefficient of the sample between the mirrors, α :

$$\gamma = \gamma_0 + \alpha c$$

where γ_0 is the decay rate of the empty cavity and c is the speed of light inside the cavity. The empty cavity decay rate is defined by the reflectivity of the mirrors, R , and the length of the cavity, L :

$$\gamma_0 = c(1 - R)/L$$

The value of γ_0 can be experimentally determined either by evacuating the cavity or by tuning the excitation laser off absorption resonance. The latter method is advantageous because it allows cancellation of the effect of Rayleigh scattering and other weakly wavelength-dependent background losses in the sample gas that are included in the measured γ_0 and automatically subtracted in the calculation of α . If the sample contribution to the cavity loss comes from a single absorbing species in the cavity, its number density in the transition level, N , can be calculated from the wavelength-dependent absorption cross section, $\sigma(\lambda)$:

$$N = \alpha(\lambda)/\sigma(\lambda)$$

Because the ring-down rate is dependent only on the properties of the resonator and the contained absorbing species, the measured number density is not affected by absorption outside the cavity. The cavity decay rate is then directly proportional to the concentration of the analyte when a well-resolved pressure-broadened line is measured, in which the absorption coefficient at the peak of the line is independent of absolute pressure.

Although CRDS is commonly implemented with pulsed lasers, it was recognized that there are several advantages to using CW laser sources.^{3,12,13} Using such a source, which typically has a narrower bandwidth than the free spectral range of the cavity, greater excitation efficiency is possible when the laser frequency is brought into resonance with a cavity mode; Appendix I discusses cavity transmission and its improvement with CW excitation. Cavity mode stability is also improved through excitation with a narrow line width TEM₀₀ mode source, thus reducing fluctuation in ring-down rates caused by the differing diffraction loss of higher-order cavity modes. Furthermore, CW diode lasers are more attractive than pulsed lasers for construction of an analytical instrument due to their low cost, simple maintenance, and ease of operation.

Distributed feedback (DFB) lasers, one popular type of diode laser, offer many advantages over other types of diode lasers for CRDS, including lower cost, greater ease of use, and a continuously tunable spectral range of up to 3 nm.¹ Additionally, they do not require moving parts for tuning, resulting in reduced sensitivity to external vibration and greater long-term stability. Unlike some other types of diode lasers, DFB lasers are easily modulated at high frequency, providing an additional advantage for CRDS

instrument construction.¹⁴ Although they have been well tested for trace gas detection, little use has been made of DFB lasers in CRDS, in part because of the high-frequency phase noise that is one of their characteristics.^{15–17}

Despite small, noisy, predicted transmission values, we demonstrate high signal-to-noise ratios and excellent absorbance sensitivity using a DFB laser. Powerful DFB lasers, capable of generating more than 1 mW, are readily available in the spectral region about 1400 nm where water exhibits relatively strong overtone transitions with line strengths on the order of 10²⁰ cm/molecule.¹⁸ We designed our CW-CRDS system to operate in this region, initially using transitions near 1322 nm for detection of concentrations on the order of parts per million by volume (ppmv) and above, and later with transitions near 1396 nm for concentrations of ppbv and below. The weaker absorption lines near 1322 nm allowed for characterization and optimization of system sensitivity without the need to achieve ultralow moisture concentrations in the ring-down cell. Sensitivity extrapolations to stronger transitions were confirmed through moisture measurement of levels as low as single ppbv at 1396 nm with a calculated noise equivalent concentration of 2 pptv, far exceeding currently reported CRDS detection levels.^{19,20}

EXPERIMENTAL SECTION

A schematic drawing of the experimental apparatus is shown in Figure 1. The resonator is excited with either a DFB laser source centered at either 1322 nm, with a fwhm of 50 MHz (model SU1322, Sensors Unlimited, Inc., Princeton, NJ), or 1396 nm, with a fwhm of 25 MHz (model SU1396, Sensors Unlimited, Inc.). The laser's wavelength is scanned through adjustment of either its temperature, for coarse changes, or its drive current, for fine-tuning. Its output is shaped with an anamorphic prism and spatially separated irises that correct astigmatism and improve spatial coherence. The laser radiation mode is then matched to the TEM₀₀ mode of the cavity by a Galilean telescope.

The shaped beam is interrupted to allow measurement of the cavity intensity with an acoustooptic modulator (AOM; model ACM-805A1, IntraAction Corp., Bellwood, IL), a common optical device.²¹ In addition to deflecting the beam from the cavity on a time scale significantly faster than the ring-down time of the cavity, the AOM allows for faster recovery than electronic current modulation of the laser.²² Also, the AOM helps to effectively isolate the diode laser from feedback reflections from the cavity by shifting the light frequency by twice the AOM drive frequency.²³

(14) Hahn, J. W.; Yoo, Y. S.; Lee, J. Y.; Kim, J. W.; Lee, H.-W. *Appl. Opt.* **1999**, *38*, 1859–1865.

(15) Romanini, D.; Kachanov, A. A.; Morville, J.; Chenevier, M. In *EnviroSense-Munich 1999*; Werner, C.; Kamermann, G., Eds.; International Congress Centre: Munich, 1999.

(16) Durry, G.; Megie, G. *Appl. Opt.* **1999**, *38*, 7342–7354.

(17) Corsi, C.; Inguscio, M.; Chudzynski, S.; Ernst, K.; D'Amato, F.; De Rosa, M. *Appl. Phys. B: Lasers Opt.* **1999**, *68*, 267–269.

(18) Toth, R. A. *Appl. Opt.* **1994**, *33*, 4851–4867.

(19) Xie, J.; Paldus, B. A.; Wahl, E. H.; Martin, J.; Owano, T. G.; Kruger, C. H.; Harris, J. S.; Zare, R. N. *Chem. Phys. Lett.* **1998**, *284*, 387–395.

(20) Romanini, D.; Lehmann, K. K. *J. Chem. Phys.* **1993**, *99*, 6287–6301.

(21) *Handbook of Optics, Volume II: Devices, Measurements, and Properties*; Bass, M., Ed. in Chief; sponsored by the Optical Society of America; McGraw-Hill: New York, 1995; p 12.26–12.29.

(22) Anderson, D. Z.; Frisch, J. C.; Masser, C. S. *Appl. Opt.* **1984**, *23*, 1238–1245.

(23) Paldus, B. A.; Harris, J. S., Jr.; Martin, J.; Xie, J.; Zare, R. N. *J. Appl. Phys.* **1997**, *82*, 3199–3204.

(12) Romanini, D.; Kachanov, A. A.; Sadeghi, N.; Stoeckel, F. *Chem. Phys. Lett.* **1997**, *264*, 316–322.

(13) Romanini, D.; Kachanov, A. A.; Stoeckel, F. *Chem. Phys. Lett.* **1997**, *270*, 538–545.

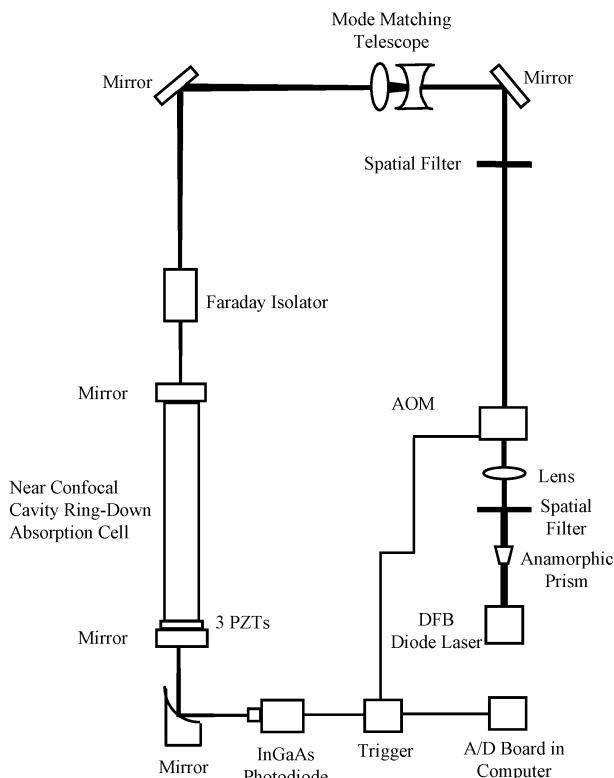


Figure 1. Schematic diagram of the CW-CRDS system.

Additional isolation is provided by a 60 dB Faraday isolator (model I-13-MM-H, Isowave, Dover, NJ) placed before the cavity that significantly reduces feedback to the laser, stabilizing its operation, and yielding more reproducible ring-down signals.

The ring-down cavity is formed by two mirrors, each 2.5 cm in diameter, with a 1-m radius of curvature, and separated by 121 or 130 cm, for experimentation at 1322 (model 10CM00SR.60F, Newport Corp., Irvine, CA) and 1396 nm (custom optics, Research Electro-Optics, Inc., Boulder, CO), respectively. The mirrors used at 1322 nm have a reflectivity of 99.985%, while those used at 1396 nm have a specified reflectivity of 99.9985%. Both ring-down systems have piezoelectric transducers (PZTs) mounted to the output mirror to allow fine control of the cavity length and resonance tuning. The mirrors form the ends of a glass cell sealed with rubber gaskets; however, for the detection of ultralow concentrations at 1396 nm, the glass cell, which limits moisture detection to 28 ppbv, is replaced with a 53-cm stainless steel cell. The mirrors used at 1396 nm are designed with a wedged substrate in order to avoid interference effects between the mirror surfaces and to stabilize ring-down rates; Appendix II discusses these effects. The mirrors used at 1322 nm do not have such a wedge, so the optical axis of the cavity is tilted relative to the mirror centers to produce a similar effect.

The cavity transmission is focused onto a 0.3-mm-diameter InGaAs detector (custom detector, Sensors Unlimited, Inc.) with amplifier (model 341-4-INV-10pf, Analog Modules, Inc., Longwood, FL) that has a noise equivalent power of 5×10^{-14} W/ $\sqrt{\text{Hz}}$ and an equivalent noise input of 0.6 nW in a 1.5-MHz bandwidth. The detector's signal is split between the AOM trigger and a 16-bit, 1-MHz analog-to-digital acquisition board (model Fast 16-1-1, Analogic Corp., Peabody, MA) on a personal computer. After it is adjusted by subtraction of a dark current offset, the digitized signal

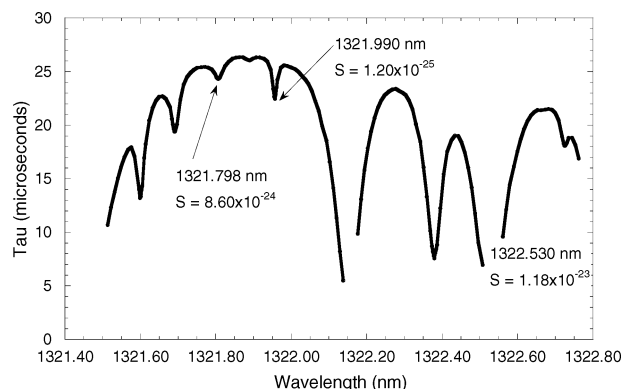


Figure 2. Moisture scan. The diode laser was scanned from 1321.50 to 1322.73 nm with ambient air in the CRDS cavity. Each data point represents the mean ring-down time from fits of 100 decays. The positions and relative intensities agree with HITRAN 92 with the exception of the line at 1321.798 nm, for which the strength is ~ 100 times too large.²⁶

is converted to a logarithmic value and fit to a first-order exponential with a weighted linear least-squares fitting routine. The use of a linear fit reduces processing time and allows for an increased sampling rate and real-time measurement.

The system was first used to confirm the reflectivity of the 1396-nm mirrors under dry nitrogen gas from the blow-off of a 250-L liquid N_2 tank. The nitrogen is passed through a molecular sieve, a purifier, and a particle filter before entering the ring-down cavity. CRDS measurements were conducted on a sample with a known quantity of water vapor in nitrogen gas, produced by a calibrated commercial moisture generator (custom generator, Meeco, Inc., Warrington, PA). The generator operated in the range between 1.4 and 11 ppmv, which was found to have an 8% accuracy. Moisture in the flow exiting the cavity was independently monitored by a commercial moisture sensor with a specified accuracy of the greater of $\pm 2\%$ of the reading or ± 20 ppbv (Aquamatic+, Meeco, Inc.). In each case, the cell was flushed for at least 30 min to remove any atmospheric moisture contribution.

RESULTS AND DISCUSSION

1322-nm System. When evacuated, the 1322-nm cavity gave a ring-down time of 31 μs , indicating mirror reflectivity of 99.987%, slightly higher than the manufacture specification of 99.985%. The locations of water absorption peaks in this spectral region are roughly determined by scanning the CW-CRDS system from 1321.50 to 1322.75 nm with ambient air in the cavity, as shown in Figure 2. Absorption peaks, indicated by a decrease in τ , are found to closely match the reported water peak locations and strengths, with one exception. Our system measured a strength 2 orders of magnitude weaker than the reported value at 1321.798 nm, indicating a possible error in the original report.²⁴

Strong absorption regions are found when the cavity is filled with ambient air that contains more than 1000 ppmv of moisture. This limits the system's sensitivity at high levels, causing increased instability in the ring-down rate.²⁵ The average ensemble standard

(24) Gianfrani, L.; De Natale, P.; De Natale, G. *Appl. Phys. B: Lasers Opt.* **2000**, *70*, 467–470.

(25) Scherer, J. J.; Paul, J. B.; O'Keefe, A.; Saykally, R. J. *Chem. Rev.* **1997**, *97*, 25–51.

deviation of γ , representing the reproducibility of absorption measurements, was 0.43% over the range from 1321.50 to 1322.73 nm, using 100 decays at each sampled wavelength. In regions where $\gamma \gg \gamma_0$, the uncertainty in the measured value of γ is increased due to reduced transmission of the cavity and fewer fitted points in the transient signal (see eq 1 of Appendix I). A significant improvement is possible when a weaker transition is measured, such as that located at 1321.99 nm, that is 2 orders of magnitude weaker than the strongest absorption resonance in the region. A measured average ensemble standard deviation of 0.14% for 100 samples at this wavelength indicates a noise equivalent absorption coefficient of $2 \times 10^{-10} \text{ cm}^{-1}$; we consider this representative of the true sensitivity of the system.

Measurements in high-purity nitrogen gas were done to determine the reproducibility of the cavity decay rate under lower concentration conditions. The fit to the ring-down transients predicted a fractional uncertainty of less than 1×10^{-4} in the ring-down rate and gave an average reduced χ^2 of 1.716, indicating that the individual transients were well described by a single-exponential fit. An ensemble standard deviation of 0.25% was measured for multiple decays, substantially higher than the statistical error estimate for an individual decay. This effect may be due to the excitation of higher-order modes in the cavity, the relative excitation of which may change between decays resulting in fluctuations in τ . Because of this, we report ensemble standard deviation values without dividing by \sqrt{n} , the number of samples, unless otherwise noted.

The accuracy of the CW-CRDS system was confirmed with experiments under controlled conditions using a calibrated moisture generator from Meeco, Inc. with the system set to monitor the water transition centered at 1322.53 nm, which has an absorption strength of $1.18 \times 10^{-23} \text{ cm}^2/\text{molecule}$ and half-width at half-maximum of 0.0707 cm^{-1} .²⁶ As the added water content was changed between 3.5 and 11 ppmv, ring-down measurements showed an average agreement with the moisture generator reading of 3.1%. With 3.5 ppmv of added moisture content, the CW-CRDS system agreed with the moisture generator to within 1.3%, reflecting improved precision at lower concentration. As the concentration of added moisture is reduced to 1.4 ppmv, the difference in γ and γ_0 becomes 0.16%, nearly the peak-to-peak noise level of the system. A plot of concentration as a function of the difference in γ and γ_0 indicates the expected linear relationship, with rms residuals in the fit allowing an uncertainty in the determination of γ of 6.5 s^{-1} over 100 decays; using this noise-equivalent rate, a minimum detectable moisture concentration of 150 ppbv can be calculated.²⁷

The minimum detectable absorbance of the system is $1.5 \times 10^{-9} \text{ cm}^{-1}/\sqrt{n}$; thus, the sensitivity is further improved by increasing the number of scans and increasing the modulation frequency of the cavity length. This was accomplished experimentally by averaging over 100 decays while modulating the PZTs on the cavity at 50 Hz to obtain a sensitivity of $2.2 \times 10^{-10} \text{ cm}^{-1}/\sqrt{\text{Hz}}$. Additional improvement could be attained with the CW-CRDS system by modulating the laser drive current at 1 kHz, corresponding to an absorbance sensitivity of $5.0 \times 10^{-11} \text{ cm}^{-1}/$

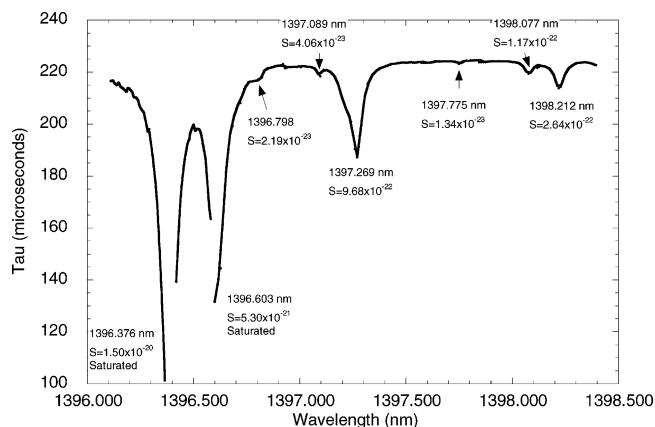


Figure 3. Moisture scan. The diode laser is scanned from 1396.100 to 1398.400 nm with 200 ppbv of moisture in the cavity. The positions and relative intensities agree with HITRAN 92 with the exception of the line at 1396.376 nm.

$\sqrt{\text{Hz}}$. This represents an improvement over other CW-CRDS systems by 2–3 orders of magnitude; compared with the only other reported DFB-based CW-CRDS system, our CW-CRDS system is 1000 times more sensitive.^{14,15,28,29}

1396-nm System. Testing of the CW-CRDS system for detection of ultralow concentrations was performed using excitation near 1396 nm, at which wavelength water absorption strengths are 3 orders of magnitude stronger than near 1322 nm. The system resolved the locations of the water peaks in this region by scanning from 1396.1 to 1398.4 nm with 200 ppbv of moisture in the ring-down cell, as shown in Figure 3. Set to an off-resonance wavelength, 1397.578 nm, a ring-down time of nearly 300 μs was observed, Figure 4. At this wavelength, the ensemble standard deviation of τ was measured to be 0.083% over 1000 ring-downs and 0.077% over 5000 decays, representing an improvement over the 1322-nm system by 1 order of magnitude in ring-down time and nearly a factor of 2 in fractional stability. The longer ring-down times, due mainly to the higher reflectivity of the 1396-nm mirrors, complement the stronger water absorption near 1396 nm

(27) The trace species concentration can be calculated using the relationships defined above for the ring-down rate as a function of the sample absorption coefficient and the number density as a function of wavelength-dependent absorption cross section. The absorption coefficient of the gas due to the analyte is given by $\Delta\gamma/c$, where $\Delta\gamma$ is the increase in ring down rate when tuning on the peak of the absorption line of the analyte and c is the speed of light. The absorption coefficient is equal to the product of the absorption cross section, σ , times the number density of the analyte. Under the conditions of our work, the absorption lines are pressure broadened and thus have a Lorentzian line shape, with fwhm given by a pressure-broadening coefficient, $\Delta\nu$, times the total sample pressure, P . For a Lorentzian line, σ at the absorption maximum can be calculated from the integrated strength of the line, S , by using the expression $\sigma = 2S/(\pi\Delta\nu P)$ with $\Delta\nu$ expressed in units of $\text{cm}^{-1} \text{ atm}^{-1}$. From these expressions, the molar concentration of the analyte in the gas can be calculated as $\Delta\gamma\pi\Delta\nu/(2SN_Lc)$, where N_L equals the number density of the gas at 1 atm of pressure at the temperature of the sample. In the pressure-broadened limit, the observable, $\Delta\gamma$, is directly proportional to the analyte concentration but independent of the sample pressure. In addition, it depends on the major composition of the gas, in that $\Delta\nu$ is dependent upon both the analyte, the specific molecular transition used, the collision partners of the analyte, and the sample temperature. The noise equivalent concentration is calculated by replacing $\Delta\gamma$ with the rms value of γ in this expression.

(28) Levenson, M. D.; Paldus, B. A.; Spence, T. G.; Harb, C. C.; Harris, J. S., Jr.; Zare, R. N. *Chem. Phys. Lett.* **1998**, *290*, 335–340.

(29) Paldus, B. A.; Harb, C. C.; Spence, T. G.; Wilke, B.; Xie, J.; Harris, J. S.; Zare, R. N. *J. Appl. Phys.* **1998**, *83*, 3991–3997.

(26) Rothman, L. S.; Gamache, R. R.; Tipping, R. H.; Rinsland, C. P.; Smith, M. A. H.; Benner, D. C.; Devi, V. M.; Flaud, J.-M.; Camy-Peyret, C.; Perrin, A.; Goldman, A.; Massie, S. T.; Brown, L. R.; Toth, R. A. *J. Quant. Spectrosc. Radiat. Transfer* **1993**, *48*, 469–507.

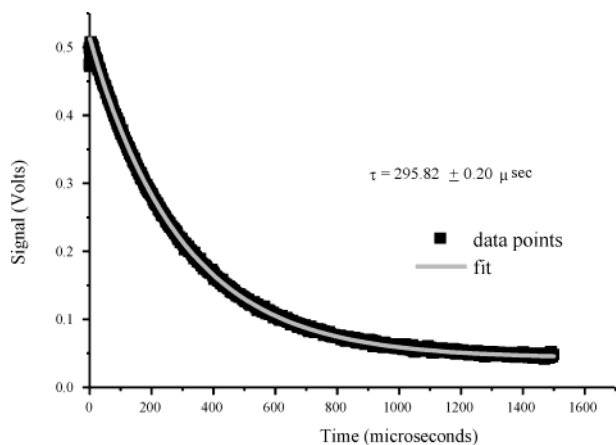


Figure 4. Ring-down decay with a 130-cm cavity purged with dry N_2 corresponding to a mirror reflectivity in the cavity of 99.99865%.

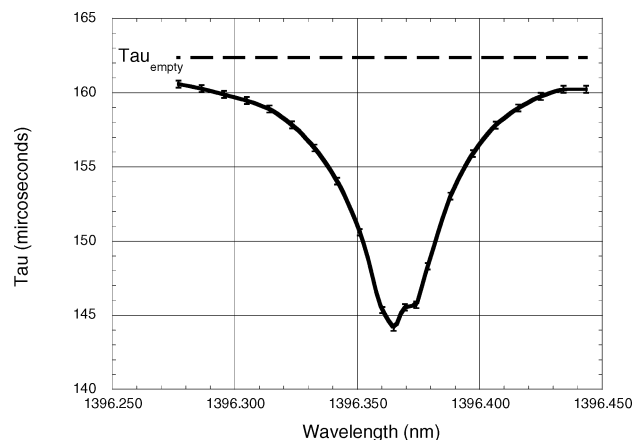


Figure 5. A 28 ppbv moisture scan. The 1396.376-nm water line is scanned using a 130-cm glass cell, and 28 ppbv of moisture is detected. Each data point consists of 10 decays, with an ensemble standard deviation of 0.15%. Data points are connected for ease of viewing and to show the Lorentzian shape of the absorption line.

to provide lower detection limits in comparison with the 1322-nm system. Furthermore, the individual ring-down times showed no evidence of statistical correlation or drift over longer acquisition periods, indicating sufficient stability for extensive averaging.

The high stability of the system enhances the sensitivity to ultralow water concentrations. Using direct measurement of 28 ppbv of moisture in a glass cell, Figure 5, the system exhibits a standard deviation in the ring-down time of 2.6 s^{-1} or 0.077% of the ring-down rate. On the 1396.376-nm water absorption line, this corresponds to a noise equivalent absorbance of $9.2 \times 10^{-11} \text{ cm}^{-1}/\sqrt{n}$ and a noise equivalent moisture concentration of 68 pptv/ \sqrt{n} . At room temperature and at pressures for which absorption lines are Doppler-limited, this means the system can detect a noise equivalent water number density of $1.4 \times 10^8 \text{ molecules cm}^{-3}/\sqrt{n}^{-1}$. Averaging over 1000 decay events, the minimum detectable moisture concentration becomes 2 pptv in nitrogen, or $4.3 \times 10^6 \text{ molecules/cm}^3$ at room temperature in a Doppler-limited matrix.

Confirmation of these sensitivity extrapolations required direct detection of concentrations below 28 ppbv, possible only with the use of a stainless steel cell. This cell was used to measure 3.85 ppbv of moisture with a standard deviation of 0.14% in τ and a difference between τ and τ_0 of 0.98%. The rms baseline noise of

$4.7 \times 10^{-10} \text{ cm}^{-1}/\sqrt{n}$ corresponds to a noise equivalent moisture concentration of 30 pptv when averaging over 50 decay events.

To determine the system's accuracy near 1396 nm, it was compared with a calibrated commercial moisture generator, capable of introducing between 88 and 200 ppbv of moisture to the ring-down cell. Good agreement was found when monitoring the water transition at 1396.603 nm, but significant deviations were discovered at the transition centered at 1396.376 nm. Concentration differences at 1396.603 nm were 7% at 90 ppbv and 1% at 100 ppbv; however, at 1396.376 nm, the differences were 20 and 30%, respectively, suggesting an error in the 1992 HITRAN database from which the moisture concentrations were calculated.²⁶ Our result agrees with the line strength reported by Toth for the 1396.376-nm line, $1.13 \times 10^{-20} \text{ cm}^{-1}/\text{molecule}$, or 25% lower than the value reported in HITRAN 92.^{18,26} We independently confirmed Toth's results by direct measurement at low vapor pressure, less than 1 Torr, in a 10-cm absorption cell.

The strengths of the various water absorption lines in the region about 1396 nm permit the further extension of the dynamic range of the CW-CRDS instrument. The absorption line at 1396.376 nm allows a dynamic detection range of $\sim 10^3 \sqrt{n}$, limited by low transmission at concentrations near the upper detection limit of 1 ppmv. However, monitoring of higher concentrations is possible by using weaker absorption lines in close spectral proximity, such as that centered at 1397.775 nm, which is 3 orders of magnitude weaker. By switching the laser as the moisture level increases to weaker transitions within its tuning range, the same instrument can be used to detect up to 1000 ppmv of water vapor, increasing the dynamic detection range to $\sim 10^7 \sqrt{n}$.

CONCLUSIONS

We have constructed a CW-CRDS system for trace gas detection using a near-infrared DFB diode laser. Even under modest gas flow conditions, the system is extremely sensitive, showing rms fluctuations in the ring-down time as low as 0.077% of the $\sim 300\text{-}\mu\text{s}$ decay time, corresponding to a minimum detectable absorption coefficient of $9.2 \times 10^{-11} \text{ cm}^{-1}/\sqrt{n}$. The cavity is also very stable over intervals as long as 5000 ring-down events, indicating the potential for extensive averaging to improve sensitivity. These specifications correspond to a noise equivalent concentration of 70 pptv/ \sqrt{n} of moisture in nitrogen gas or 2 pptv when averaging 1000 decay rates at 1396.376 nm. The system's dynamic range can be extended to water vapor concentrations as high as 1000 ppmv by monitoring several absorption lines of different strengths within the spectral scanning range of the laser.

The present design is suited for development of a practical industrial trace gas sensor, in large part because of the versatility of the DFB laser source. The instrument described in this work is the basis for the design of the first commercial CRDS instrument, specified to detect 100 pptv of H_2O in N_2 .³⁰ While this work has focused on trace sensing of moisture, only small changes in the detection wavelength are required to measure a number of other small hydride species at similar detection levels, including methane, acetylene, and ammonia.

(30) MTO-1000- H_2O . http://www.tigeroptics.com/pdf/MTO_1000_H2O.pdf; accessed 2003.

ACKNOWLEDGMENT

The authors thank Dr. Wen-Bin Yan for helpful discussions; the New Jersey Commission on Science and Technology, the National Science Foundation, and Meeco, Inc. for financial support of this work; and Sensors Unlimited for generous donation of custom equipment.

APPENDIX I

In comparison to a resonator excited by a pulsed laser, the peak transmission of a CW-CRDS cavity, T_c , is enhanced by a factor approximately equal to the ratio of the cavity-free spectral range to the laser's full width at half-maximum (fwhm). If the transverse mode of the excitation radiation is matched to that of the cavity, the time-averaged transmission of the laser through the cavity, and the detected signal intensity at the start of the ring-down curve, can be derived by convolution of the frequency-dependent transmission of a cavity, previously given in ref 32, with a laser line shape that is assumed to be Lorentzian. The transmission, T_c , is expressed as

$$T_c = \left(\frac{T}{1-R}\right)^2 \left(\frac{\gamma_0}{\gamma}\right)^2 \left(\frac{\gamma}{\gamma + 2\pi\Delta\nu_L}\right)^2 \quad (1)$$

in which T is the transmission of the cavity mirrors, R is their reflectivity, γ is the cavity ring-down rate, γ_0 is the empty cavity ring-down rate, and $\Delta\nu_L$ is the fwhm of the laser emission spectrum. The first factor can approach unity, but it is limited by the loss in the mirror coatings and is generally kept at ~ 0.5 for the high-quality mirrors used in CRDS. The γ_0/γ factor is nearly unity for weak absorption, although it can significantly depress the cavity transmission if the absorption per pass is greater than the mirror loss, thus limiting the signal-to-noise ratio of each detected ring-down transient at high concentrations or with strong absorbers. The last factor arises from the convolution of the laser line width with that of the cavity. Technological improvements that lead to the reduction of laser line width can be expected to enhance system sensitivity because of improved selectivity in transverse cavity mode excitation and the resulting increased cavity throughput.

Numerical modeling of the fluctuations in cavity transmission, assuming random Gaussian phase noise, demonstrates that the cavity transmission is similar to laser "speckle noise", in which transmission is modulated from zero to its peak value, nearly 1 order of magnitude about the time-averaged value.³¹ This effect arises because the light fields add incoherently if they enter the cavity at times separated by more than the coherence time of the laser. The central limit theorem implies that when the laser coherence time is much less than the cavity ring-down time, the real and imaginary components of the electric field are both Gaussian random variables, and thus, the laser intensity will follow a χ^2 distribution in two degrees of freedom. Thus, the probability of having instantaneous transmission, I , is described by $\exp(-I/\langle I \rangle)$, where $\langle I \rangle$ is the time-averaged value of transmitted intensity. Additionally, the transmission is modulated on time scales as short as the coherence time of the laser, but it has a $1/e$ correlation time equal to the cavity decay time.

The time-averaged cavity transmission expression assumes centering of the mean laser frequency over the resonance of the cavity. However, the buildup of radiation inside the cavity, and thus the peak transmission intensity, is experimentally reduced because of the finite difference between cavity resonance and laser frequency. Low-frequency jitter, either in the laser or due to mechanical instabilities of mirror separation, also contributes to this reduction. Ziyuan et al. analyzed cavity transmission in this non-time-averaged case.³¹ Evaluation of their integral expression by the method of steepest descent, ignoring fast jitter, gives an expression for the peak transmission of the cavity:

$$T_c = \left(\frac{T}{1-R}\right)^2 \gamma_0^2 \left(\frac{\delta\nu}{\delta t}\right)^{-1} \quad (2)$$

in which $\delta\nu/\delta t$ is the rate of frequency sweep over the cavity resonance. At a sweep rate of $\sim 10^{11}$ Hz/s, corresponding to sweeping the cavity over one free spectral range 10^3 times/s, the finite sweep rate will reduce T_c by nearly 4 orders of magnitude compared with monochromatic excitation of the cavity. Using phase diffusion to account for the spectrum of the laser, numerical calculations demonstrate that the peak transmission is approximated by the smaller of the transmission values predicted by eqs 1 and 2. In comparison with the reduction of cavity transmission dominated by laser jitter, fluctuations in peak cavity transmission are significantly reduced when resonance sweep makes the primary contribution.

APPENDIX II

Significant fluctuation was initially found in the fitted ring-down rates due to Newton's rings, which are interference effects between the highly reflecting spherical surfaces and the flat anti-reflection (AR)-coated back of the mirror substrates. This interference leads to an effective modulation of cavity reflectivity with a period of $c/(2nd)$, where n is the refractive index of the mirror substrate and d is its thickness.²⁰ The relative phase of the interfering fields is affected by fluctuations in temperature, laser alignment, or beam position at the cavity input, and it can alter the mirror's effective reflectivity and consequently the ring-down rate.

We eliminate this effect by introducing a wedge in the mirror substrate sufficient to remove overlap between the interfering reflections. The 1322-nm mirrors used in this work are not adequately wedged, but the 1396-nm mirrors are. At normal incidence, we observed a 3% variation in the transmission as a function of displacement from the optic axis, consistent in shape with Newton's rings. To avoid this problem, the 1322-nm cavity is aligned in a somewhat unconventional way. Normally, to minimize diffraction loss, one aligns the cavity such that the optical axis is centered on the optics. In the present case, off-axis alignment is possible because the Fresnel number, ~ 400 , is large. The optic axis is moved ~ 0.6 cm closer to an edge of the input mirror and closer to the opposite edge of the output mirror, in effect skewing the axis through the resonator. As a result, light enters off-center and away from normal incidence to the plane mirror surface, causing the interference effects to disappear. By tilting the optical axis through the resonator, the mirrors are effectively wedged.

An AR coating as good as 0.01% can lead to effective mirror reflectivity modulations on the order of 1%, which significantly

(31) Ziyuan, L.; Bennett, R. G. T.; Stedman, G. E. *Opt. Commun.* **1991**, *86*, 51-57.

compromises CRDS sensitivity and requires wedged mirrors.²⁰ The reflectivity modulation can be described by treating a single mirror as an asymmetric etalon having a highly reflective coated surface, with intensity reflectivity R_1 , and an uncoated or AR-coated surface, with intensity reflectivity R_2 . For CRDS mirrors, for which R_1 is approximately equal to 1, and R_2 is significantly less than 1, the effective reflectivity of the compound reflector, R_{eff} , can be described by

$$1 - R_{\text{eff}} = (1 - R_1) - 2T_1\sqrt{R_2}A \sin(4\pi d/\lambda) \quad (3)$$

where d is the optical thickness of the mirror, λ is the wavelength of the radiation, A is the amplitude of the overlap between the reflections from the two surfaces, and T_1 is the transmission of the highly reflective surface, which is approximately equal to $(1 - R_1)$. For a highly reflective surface with a radius of curvature, R_c , the reflected wave from this surface will have a radius of curvature, $-R_c$; after reflection off a flat, low-reflectivity surface and propagation back through the highly reflective surface on a

substrate with a refractive index, n , the curvature of the wave becomes $R_c/(2n - 1)$. The modal overlap of this wave with the TEM₀₀ mode of the cavity is given by³²

$$A = \left[\frac{1}{1 + (\pi\omega^2 n/\lambda R_c)^2} \right] \approx \frac{1}{1 + n^2} \quad \text{for a near confocal cavity} \quad (4)$$

where ω is the mode spot size on the mirror. Slightly wedged optics help to avoid these interference effects in CRDS. For a planar reflector with a wedge angle of $\delta\theta$ in radians, we calculate the amplitude of the overlap due to the wedge as³²

$$A = \exp[-2\pi^2(\omega n\delta\theta/\lambda)^2]$$

This expression can be used to estimate the minimum wedge needed to reduce the overlap to an acceptable level. In our CW-CRDS system, this corresponds to a wedge angle of ~ 2 mrad to reduce the overlap amplitude to less than 10^{-4} .

Received for review March 27, 2003. Accepted June 15, 2003.

AC0343073

(32) Lehmann, K. K.; Romanini, D. *J. Chem. Phys.* **1996**, *105*, 10263–10277.